World Journal of Pediatric Surgery

CT manifestations of childhood pancreatoblastoma

Meijun Sheng,[1] Ruifang Zhang,[2] XiaoHui Ma,[2] Haichun Zhou [2]

To cite: Sheng M, Zhang R, Ma X, *et al*. CT manifestations of childhood pancreatoblastoma. *World Jnl Ped Surgery* 2022;**5**:e000398. doi:10.1136/wjps-2021-000398

Received 26 November 2021
Accepted 27 April 2022

[1]Surgical Intensive Care Unit, Zhejiang University School of Medicine Children's Hospital, Hangzhou, Zhejiang, China
[2]Department of Radiology, Zhejiang University School of Medicine Children's Hospital, Hangzhou, Zhejiang, China

Correspondence to
Dr Haichun Zhou; zjzhc815@zju.edu.cn

Pancreatoblastoma is the most common type of malignant pancreatic tumor in children under 10 years old, accounting for 25% of pancreatic tumors.[1] The imaging findings of pancreatoblastoma are non-specific, and most of tumors are lobulated masses with well-circumscribed or partially circumscribed margins, accompanied by necrosis and enhancing septations on contrast-enhanced CT.[2] When a large tumor originates in the pancreas, pancreatoblastoma is one of the top differential diagnoses in children because of its relative frequency in this age group.[3] However, owing to the usual tumor's large size at diagnosis, a tumor originating from the pancreas may be misdiagnosed with a tumor originating from a peripancreatic organ, such as neuroblastoma, lymphoma, or hepatoblastoma. The differential diagnosis in these tumors is more challenging, and the potential for misdiagnosis still exists. Therefore, it is important to delineate the origin of tumor clearly on CT. The present study analyzed the imaging CT findings of pancreatoblastoma retrospectively.

The inclusion criteria were as follows: (1) patients diagnosed as pancreatoblastoma by pathology; (2) complete CT information including that from non-contrast and contrast CT. The exclusion criteria were as follows: patients with no complete CT information or pathological diagnosis. In this study, four patients with pancreatoblastoma who underwent tumor biopsy and three patients who had tumor resection from January 2014 to March 2020 were analyzed retrospectively. The diagnosis of pancreatoblastoma was based on the analyzed examination, which revealed that the acinar and trabecular areas were associated with the nests of squamous epithelium (squamoid nests), and the immunohistochemical staining which showed CK (+) and AAT (+). A second review of the specimens for the scope of the study was done by a gastrointestinal pathologist with 12 years of experience in gastrointestinal pathology.

All CT examinations were performed on a 64-slice CT scanner (Optima CT660; GE Healthcare). The scan parameters were as follows: 80–100 kVp, 40–70 mA current, 5 mm thickness, and 1.375 pitch. The contrast medium Iohexol (Hengrui Medicine, Jiangsu, China) was injected by a high-pressure syringe at a dose of 1.5–2 mL/kg and a rate of 1–2 mL/s through the cubital vein. The 3D volume-rendered or maximum intensity projection reconstruction method was used to display the tumor's feeding arteries and peritumoral blood vessels.

CT images were analysed independently by two radiologists who had 5 and 17 years of experience in pediatric abdominal CT. These radiologists were aware of the diagnosis of pancreatoblastoma but were blinded to the surgical and pathologic details. If there was any doubt or dispute, a third senior radiologist with 20 years of experience in pediatric abdominal CT was consulted to reach an agreement. The following features were analyzed: tumor origin (head, body or tail), tumor size (largest axial diameter), tumor shape (oval or round, lobulated, irregular), tumor margin (clear or indistinct), tumor encapsulation (complete, incomplete, and no visible encapsulation), tumorous cystic solidity (mainly cystic, mixture of cystic and solid, and mainly solid), calcification (present or absent), intratumoral vessels (present or absent), invasion of adjacent structures (present or absent), tumor-feeding arteries, and the spatial relationship between the tumor and surrounding organs and blood vessels.

Based on the proportion of the cystic component, the tumor was categorized into mainly cystic (cystic component of >70%), mainly solid and cystic (cystic component of 30%–70%), or mainly solid (cystic component of <30%). Vascular invasion was defined as vessel occlusion, stenosis, or contour deformity associated with tumor involvement. A feeding artery was defined as a hypertrophied artery that ran in accordance with the shape

Table 1 Clinical and imaging findings in seven children with pancreatoblastoma

	Case 1	Case 2	Case 3	Case 4	Case 5	Case 6	Case 7
AFP level (0–20 ng/mL)	32.5	31.4	155.7	319.4	380.6	0.9	1.2
Clinical presentation	Abdominal pain	Palpable mass	Palpable mass	Vomiting, palpable mass	Abdominal pain, distention, palpable mass	Abdominal pain	Fever, palpable mass
Tumor location	Tail	Head	Body	Body/tail	Body/tail	Body	Head
Encapsulation	Incomplete	Incomplete	Complete	Incomplete	Incomplete	Complete	Complete
Morphology	Irregular	Irregular	Lobulated	Lobulated	Lobulated	Lobulated	Lobulated
Margin	Partly indistinct	Partly indistinct	Clear	Clear	Clear	Clear	Clear
Size (cm)	6.7	7.7	7.2	12.5	14.5	9.2	10
Heterogeneity	Cystic-solid	Mainly solid	Cystic-solid	Mainly cystic	Mainly cystic	Mainly cystic	Cystic-solid
Calcification	Curvilinear and punctate	Curvilinear and punctate	Curvilinear and punctate	Curvilinear and punctate	Curvilinear and punctate	Punctate	Curvilinear and punctate
Contrast enhancement	Heterogeneous	Heterogeneous	Heterogeneous	Heterogeneous	Heterogeneous	Heterogeneous	Heterogeneous
Invasion	Yes	Yes	No	Yes	Yes	No	No
Feeding artery	SA	GDA, SMA	GDA, SMA	GDA, SA, SMA, LGA, RGA	SA, SMA	GDA, SA	GDA, SMA

AFP, alpha-fetoprotein; GDA, gastroduodenal artery; LGA, left gastric artery; RGA, right gastric artery; SA, splenic artery; SMA, superior mesenteric artery.

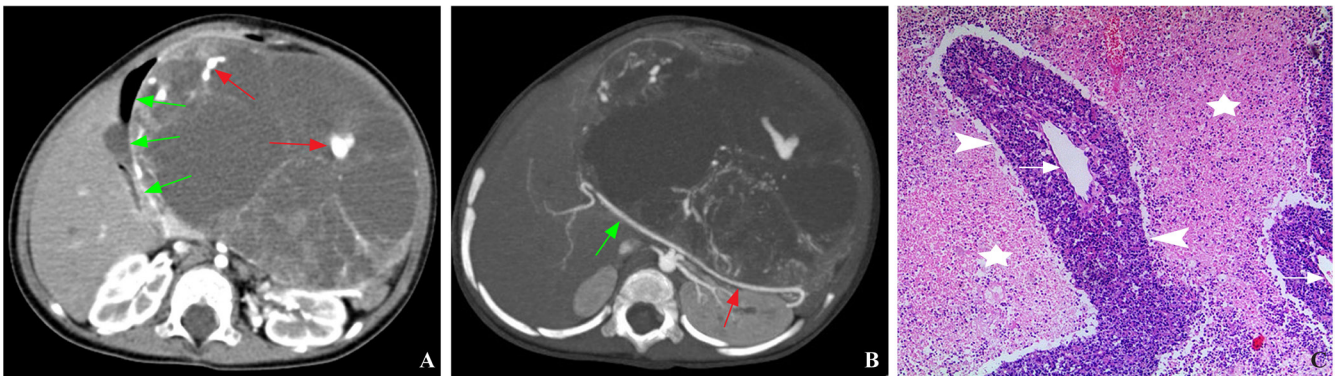

Figure 1 Pancreatoblastoma of the pancreas body and tail. (A) Axial contrast-enhanced image shows the dilatation of tumor blood vessels (red arrows) around the cystic area, and outward displacement of the second segment of the duodenum (green arrows). (B) Transverse contrast-enhanced maximum intensity projection image shows that the common hepatic artery (green arrow) is pushed backwardly and outwardly, and the splenic artery (red arrow) is pushed backwardly. (C) Pathology illustration (original magnification, ×50; H&E stain) shows a small number of tumor cells located (arrowheads) around the expanded tumor blood vessels (arrows), and large hemorrhagic necrosis (asterisks) around the tumor cells.

of the tumor with its main trunk or branches extending into the tumor body and distributed in a mesh or radial pattern. Data were presented as mean±SD. Kappa analysis was used to assess interobserver reliability. P<0.05 was defined as statistically significant. All statistical analyses were conducted using SPSS V.17.

A total of seven children (mean age was 51±23 months) were included in this study. The clinical, laboratory and CT findings are listed in table 1. In our series, palpable abdominal mass (five of seven) was the most common presenting symptom, and the serum alpha-fetoprotein (AFP) values were increased in five patients, with a mean value of 183.9±161.3 ng/mL. The resectability depends on the tumor location in the pancreas and the presence of metastasis. Four of our patients with unresectable tumor (cases 1, 2, 4 and 5) underwent tumor biopsy and received preoperative chemotherapy that allowed following surgical removal, and three patients had primary surgical resection. Types of surgery included the pancreaticoduodenectomy (cases 2 and 7), splenic-preserving distal pancreatectomy (cases 4 and 5), distal pancreatectomy with elective splenectomy (case 1) and central pancreatectomy with Roux-en-Y end-to-end pancreatojejunostomy (cases 3 and 6). Invasion of adjacent tissues and organs was detected in four cases during surgery, including the spleen (n=1), duodenum and colon (n=1), and vessels (n=3). All patients received postoperative chemotherapy. At the time of the analysis, five patients remained alive, having survived for 22, 53, 80, 105 and 124 months, one of which (case 2) relapsed after 15 months of surgery and received the second surgery.

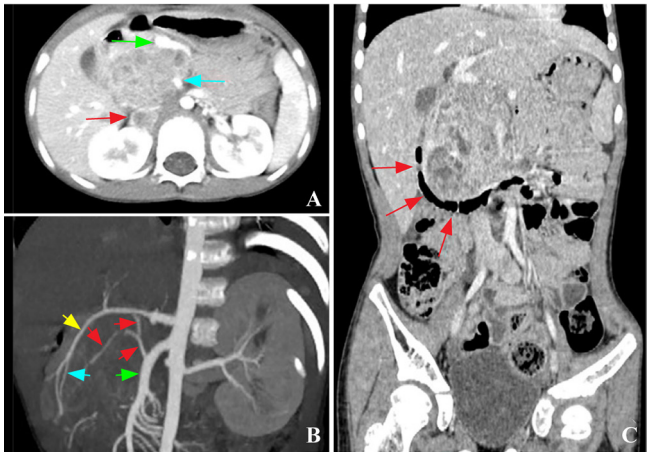

Figure 2 Pancreatoblastoma of the pancreas head. (A) Axial contrast-enhanced image shows the tumor-invaded inferior vena cava (red arrow), with the superior mesenteric vein (green arrow) and artery (blue arrow) pushed inwardly and forwardly, while the distance between the two increases. (B) Oblique coronal maximum intensity projection image shows the two feeding arteries (red and blue arrows) from the superior mesenteric artery (green arrow) and the gastroduodenal artery (yellow arrow), respectively. (C) Coronary reconstruction image shows that the mass pushes the second segment (red arrows) of the gas-containing duodenum outwardly to form an arc.

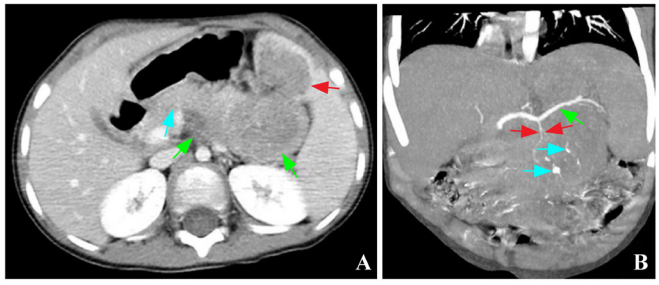

Figure 3 Pancreatoblastoma of the pancreas tail. (A) Axial contrast-enhanced image shows the mass invades the anterior part of the spleen (red arrow) and protrudes toward retroperitoneum (green arrows), with the pancreas (blue arrow) pushed forward. (B) Coronal contrast-enhanced maximum intensity projection image shows the tumor-feeding artery (red arrows) originating from the splenic artery (green arrow), and the punctate and curvilinear calcifications inside the tumor (blue arrows).

Two patients were lost to follow-up at 120 and 134 months after surgery.

In this study, all seven tumors showed exogenous growth, encapsulation, heterogeneous appearance, and calcifications on imaging. Tortuous feeding arteries in/around the tumors were seen after contrast enhancement, and cystic dilated tumor vessels were observed in three cases with mainly cystic tumors. The tumor-feeding arteries included the superior mesenteric artery, the gastroduodenal artery, the splenic artery, and the left and right gastric arteries. Four tumors directly invaded the surrounding tissues and organs. Vascular invasion was found in three cases, vascular encasement in two cases, and spleen invasion in one case.

All tumors pushed the peritumoral blood vessels and/or the second segment of the duodenum in different directions. The pancreatic head tumors pushed the superior mesenteric artery and vein inwardly while increasing the distance between them, with the second segment of the duodenum pushed outwardly in an arc shape. The pancreatic body and tail tumors were accompanied by posterior displacement of the splenic artery, posterior and outward displacement of the mesenteric artery and vein, and the outward movement of the second segment of the duodenum to form an arc shape. The pancreatic tail tumor pushed the splenic artery upward and posteriorly, and there was only mild posterior displacement of the superior mesenteric vein in cases 3 and 6 with tumors in the pancreatic body. The representative images are presented in figures 1–3.

Kappa analysis was used to evaluate interobserver reliability. For all qualitative features (origin, shape, margin, encapsulation, tumorous cystic solidity calcification, intratumoral vessels, invasion of adjacent structures, tumor-feeding arteries and spatial relationship between the tumor and surrounding organs and blood vessels), k values were all good (k=0.76–1.0, p<0.001).

Pancreatoblastoma is a slow-growing tumor and the clinical presentation can be non-specific. When physical examination shows an asymptomatic mass in the upper abdomen accompanied by elevated AFP, pancreatoblastoma should be considered.[4] Our study reveals that palpable mass accompanied by elevated AFP was present in 57.1% cases.

The diagnosis of pancreatoblastoma could be established with CT and MRI, which could clearly demonstrate the size, shape, and characteristic of the lesion. Pancreatoblastoma is often manifested as a lobulated, heterogeneous mass at CT and low-to-intermediate signal intensity on T1-weighted images and high signal intensity on T2-weighted images at MRI.[5] Our findings in this study confirmed and extended previous observations.

The density of pancreatoblastoma is heterogeneous.[6] In our study, most tumors showed mainly cystic or both solid and cystic appearance on CT. Our pathology confirmed that such cystic changes on CT reflected the bleeding, necrosis, and cystic degeneration inside the tumor. We found three tumors with mainly cystic appearance displayed the cystic expansion of the tumor vessels following contrast enhancement. We speculated that the vessel dilatation may be caused by tumor desmoplasia or post-necrotic fibrosis leading to vessel retraction because we found pathologically that these dilated blood vessels always appeared around the cystic compartments secondary to hemorrhagic necrosis of tumor cells, whereas non-dilated blood vessels were around the tumor cells that appeared intact.

Horie *et al* subdivided pancreatoblastoma into two categories on the basis of anatomic origin: right-sided tumors (head of the pancreas) arising from the pancreatic ventral anlage and left-sided tumors (body and tail of the pancreas) arising from the pancreatic dorsal anlage.[7] Many investigators have reported that right-sided tumors are usually well encapsulated, non-calcified, and generally have a good prognosis, whereas left-sided tumors lack encapsulation, exhibit calcification, and generally have a relatively poor prognosis.[7 8] In the present study, one of the two cases with right-sided tumors showed incomplete encapsulation with involvement of the peripheral blood vessels. In contrast, in the five patients with left-sided tumors, three showed incomplete encapsulation with involvement of adjacent structures. These results indicated that left-sided tumors are more aggressive than right-sided tumors which may explain the poor prognosis of patients with left-sided tumors. However, all of the patients in our study had an excellent prognosis and a high 5-year survival rate regardless of tumor anatomic origin.

We attempted to ascertain the origin of the tumor by observing the displacement of the surrounding blood vessels and organs. Our research indicated that tumor location in the pancreas should be considered when the following signs are found: (1) inward and anterior displacement of the superior mesenteric artery and vein with the increased distance between them as well as the lateral displacement of the second segment of the duodenum can be used to characterize pancreatic head pancreatoblastoma; (2) posterior displacement of the splenic artery and invasion of the splenic vessels, with or without posterolateral displacement of the superior mesenteric artery and vein, is the characteristic of pancreatic body and/or pancreatic tail pancreatoblastoma.

There have been reports of determining the origin of pelvic masses with the aid of feeding arteries.[9] However, few reports have described the feeding arteries of pancreatoblastoma. The results of this study showed that the feeding arteries of pancreatoblastoma are the same as those of the normal pancreas, namely gastroduodenal artery, the superior mesenteric artery and the splenic artery. It may be a valid hypothesis for a future study that when a

tumor's feeding artery is originated from the blood supply of pancreas, the origin of the tumor may be the pancreas.

The radiological differential diagnosis of pancreatoblastoma includes a tumor originating from a peripancreatic organ, such as hepatoblastoma, lymphoma, or neuroblastoma, and a tumor originating from the pancreas itself, which mainly includes solid pseudopapillary neoplasm. When hepatoblastoma grows into the lesser sac, it may be difficult to distinguish between hepatoblastoma and pancreatoblastoma because of similarities in age of onset, CT manifestations, and AFP elevation. However, hepatoblastoma often has a hepatic artery blood supply,[10] which may help in differentiating between the two diagnoses. Lymphoma often involves multiple organs, without calcification, and necrosis and bleeding are rare. Retroperitoneal neuroblastoma generally grows along the sympathetic nerve chain, lymph node metastasis is more common, with possible invasion of the spinal canal. In addition, retroperitoneal neuroblastoma often pushes the splenic artery forward, which is opposite to that of pancreatoblastoma. Solid pseudopapillary neoplasms often occur in females over 10 years, and calcification and aggressive growth are rare.

In conclusion, pediatric pancreatoblastoma usually appears as an exogenous, calcified, heterogeneous and hypovascularized mass with a lobulated shape on CT. Pediatric pancreatoblastoma may show aggressive growth, with localized vascular or tissue invasion. When the tumor of pancreatoblastoma is large, the origin of the tumor may be determined by observing the supplying arteries and the signs of displacement of duodenal and surrounding blood vessels.

Contributors MS contributed to writing (original draft) and data curation. RZ contributed to writing (review and editing). XM contributed to data curation and formal analysis. HZ contributed to conceptualization and supervision. No author serves as a current editorial team member for this journal.

Funding The authors have not declared a specific grant for this research from any funding agency in the public, commercial or not-for-profit sectors.

Competing interests None declared.

Patient consent for publication Not required.

Ethics approval This study involves human participants and was approved by Zhejiang University School of Medicine Children's Hospital Committee on Clinical Investigation (2021-IRB-087). This study was a retrospective analysis and did not require formal consent.

Provenance and peer review Not commissioned; externally peer reviewed.

Data availability statement The data that support the findings of this study are available from the corresponding author upon reasonable request.

ORCID iD

Haichun Zhou http://orcid.org/0000-0002-5095-9661

REFERENCES

1 Lee YJ, Hah JO. Long-term survival of pancreatoblastoma in children. *J Pediatr Hematol Oncol* 2007;29:845–7.
2 Lee JY, Kim IO, Kim WS, *et al*. CT and US findings of pancreatoblastoma. *J Comput Assist Tomogr* 1996;20:370–4.
3 Yang X, Wang X. Imaging findings of pancreatoblastoma in 4 children including a case of ectopic pancreatoblastoma. *Pediatr Radiol* 2010;40:1609–14.
4 Huang Y, Yang W, Hu J, *et al*. Diagnosis and treatment of pancreatoblastoma in children: a retrospective study in a single pediatric center. *Pediatr Surg Int* 2019;35:1231–8.
5 Yang Z, Gong Y, Ji M, *et al*. Differential diagnosis of pancreatoblastoma (PB) and solid pseudopapillary neoplasms (SPNs) in children by CT and MR imaging. *Eur Radiol* 2021;31:2209–17.
6 Montemarano H, Lonergan GJ, Bulas DI, *et al*. Pancreatoblastoma: imaging findings in 10 patients and review of the literature. *Radiology* 2000;214:476–82.
7 Horie A, Yano Y, Kotoo Y, *et al*. Morphogenesis of pancreatoblastoma, infantile carcinoma of the pancreas: report of two cases. *Cancer* 1977;39:247–54.
8 Herman TE, Siegel MJ, Dehner LP. CT of pancreatoblastoma derived from the dorsal pancreatic anlage. *J Comput Assist Tomogr* 1994;18:648–9.
9 Li Y, Zheng Y, Chen J, *et al*. Determining the organ of origin of large pelvic masses in females using multidetector CT angiography and three-dimensional volume rendering CT angiography. *Eur Radiol* 2015;25:1032–9.
10 Xuewu J, Jianhong L, Xianliang H, *et al*. Combined treatment of hepatoblastoma with transcatheter arterial chemoembolization and surgery. *Pediatr Hematol Oncol* 2006;23:1–9.